Int J Adv Manuf Technol (2010) 46:1119–1132
DOI 10.1007/s00170-009-2171-z

ORIGINAL ARTICLE

An experimental investigation of cylindrical wire electrical discharge turning process

Mohammad Jafar Haddad · Fereshteh Alihoseini · Mostafa Hadi · Meysam Hadad · Alireza Fadaei Tehrani · Aminollah Mohammadi

Received: 14 January 2009 / Accepted: 10 June 2009 / Published online: 28 June 2009
© Springer-Verlag London Limited 2009

Abstract The cylindrical wire electrical discharge turning (CWEDT) process was developed to generate precise cylindrical forms on hard, difficult to machine materials. A precise, flexible, and corrosion-resistant submerged rotary spindle was designed and added to a conventional five-axis CNC wire electrical discharge machine (EDM) to enable the generation of free-form cylindrical geometries. The hardness and strength of the work material are no longer the dominating factors that affect the tool wear and hinder the machining process. In this study, the effect of machining parameters on surface roughness (R_a) and roundness in cylindrical CWEDT of a AISI D3 tool steel is investigated. The selection of this material was made taking into account its wide range of applications in tools, dies, and molds and in industries such as punching, tapping, reaming, and so on in cylindrical forms. Surface roughness and roundness are chosen as two of the machining performances to verify the process. In addition, power, pulse off-time, voltage, and spindle rotational speed are adopted for evaluation by full factorial design of experiments. In this case, a $2^2 \times 3^2$ mixed full factorial design has been selected considering the number of factors used in the present study. The main effects of factors and interactions were considered in this paper, and regression equations were derived using response surface methodology. Finally, the surfaces of the CWEDT parts were examined using scanning electron microscopy (SEM) to identify the macro-ridges and craters on the surface. Cross sections of the EDM parts were examined using the SEM and microhardness tests to quantify the sub-surface recast layers and heat-affected zones under specific process parameters.

Keywords CWEDT · Surface roughness · Roundness · DOE

M. J. Haddad (✉) · A. F. Tehrani · A. Mohammadi
Manufacturing Engineering Division,
Department of Mechanical Engineering,
Isfahan University of Technology,
Isfahan, Iran
e-mail: m.j.hadad@gmail.com

F. Alihoseini
Statistical Science Division, Mathematical Science Department,
Isfahan University of Technology,
Isfahan, Iran

M. J. Haddad · M. Hadi
Manufacturing Engineering Division, Islamic Azad University,
Branch of Dehaghan,
Isfahan, Iran

M. Hadad
Agricultural Economics Group,
Ramin Agricultural and Natural Resources University,
Ahvaz, Iran

1 Introduction

Electrical discharge wire cutting, more commonly known as wire electrical discharge machining (WEDM), is a spark erosion process used to produce complex 2D and 3D shapes through electrically conductive workpieces by using wire electrode. The sparks will be generated between the workpiece and a wire electrode flushed with or immersed in a dielectric fluid. Good accuracy and fine surface finishes make WEDM particularly valuable for machining of stamping dies, extrusion dies, and prototype parts. These sparks generate craters and the recast layer on the surface of the electrical discharge machine (EDM) workpiece. Without WEDM, the fabrication of precise workpieces requires many hours of manual grinding and polishing [1]. The concept of CWEDT is illustrated in Fig. 1 [2]. A rotary axis is added to a conventional five-axis wire EDM machine in order to produce cylindrical forms. The initial shape of the

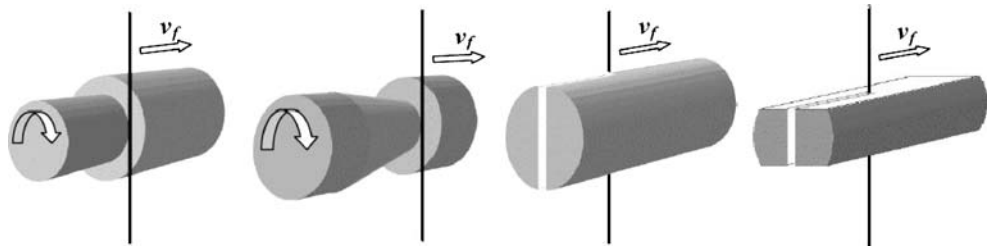

Fig. 1 The concept of turning with wire EDM and 2D wire EDM [2]

part need not be of cylindrical form. The electrically charged wire is controlled by the X and Y slides to remove the work material and generation of the desired cylindrical form [3, 4]. Some turning wire EDM works have been reported for manufacturing small pins by Masuzawa's research group at The University of Tokyo [5–7]. The small diameter pins can be used as tools for 3D micro-EDM application [8]. Examples of the machined parts using the cylindrical wire EDT method are shown in [2–4].

The application of a water-cooled submerged spindle extends the application of WEDM to WEDM turning with rotation speed up to 2,800 rpm. This enables the production of gear wheels with integrated shaft for easy gear assembly [9]. The feasibility of using cylindrical WEDM for dressing a rotating metal bond diamond wheel (used for precision form grinding of ceramics) has also been studied [10]. The results show that the WEDM process is capable of generating precise and intricate profiles with small corner radii, but a high wear rate is observed on the diamond wheel during the first grinding pass. Such an initial high wheel wear rate is due to the over protruding diamond grains, which do not bond strongly to the wheel after the WEDM process [11]. Qu et al. [3] investigated through a mathematical model the surface roughness of CWEDT parts. Mohammadi et al. [12] investigated the turning by wire electrical discharge machining to evaluate the effects of machining parameters on surface roughness and roundness. There are also a number of published works that solely study the effects of the machining parameters on the WEDMed surface. Gokler and Ozanozgu [13] studied the selection of the most suitable cutting and offset parameter combination to get a desired surface roughness for a constant wire speed and dielectric flushing pressure. Tosun et al. [14] investigated the effect of the pulse duration, open circuit voltage, wire speed, and dielectric flushing pressure on the WEDMed workpiece surface roughness. Anand [15] used a fractional factorial experiment with an orthogonal array layout to obtain the most desirable process specification for improving the WEDM dimensional accuracy and surface roughness. Spedding and Wang [16] optimized the process parameter settings by using artificial neural network modeling to characterize the WEDMed workpiece surfaces, while Williams and Rajurkar [17] presented the results of the current investigations into the characteristics of WEDM-generated surfaces. Rajurkar and Pandit [4] have studied the recast layer and heat-affected zones (HAZ) of EDM surfaces and developed a thermal model to predict the thicknesses of damaged layers. For the die sinking EDM process, the depth of the damaged layer was reported to be from 30 to 100 μm for an AISI 4130 steel workpiece machined with pulse on-time of 100 to 300 μs. Anon [4] has studied the sub-surface HAZ and recast layers of steel and tungsten carbide using the die sinking EDM and has summarized and explained the possible causes for EDM surface defects. Qu et al. [4] have studied the sub-surface

Fig. 2 Spindle in the five-axis CNC wire EDM machine

Fig. 3 A sample of punches used for machining with CWEDT process

Table 1 Chemical composition of AISI D3 tool steel

Alloy	C	Si	Mn	P	S	Cr
Quantity (%)	1.9–2.2	0.1–0.4	0.15–0.45	0.03	0.03	11–12

HAZ and recast layers of carbide and brass in cylindrical wire EDM. Under high material removal rate, 14 μs pulse on-time, a recast layer of about 3 μm thick can be clearly recognized on the surface of carbide parts. Thinner recast layers, less than 2 μm, exist on samples machined using shorter pulse on-time. Bubbles can be identified in the recast layers of carbide samples. The depth of the heat-affected zone is estimated to be about 4, 3, and 2 μm on the carbide samples with 14, 5, and 2 μs pulse on-time, respectively. Also, very thin recast layers, about 1 μm, can be observed on the cross section of three brass samples. No HAZ was observed on brass samples, possibly due to the good thermal conductivity of brass. The heat-affected zone may exist but cannot be identified in brass samples.

The objective of the mathematical models is to achieve higher machining productivity with a desired accuracy and surface finish. However, the selection of cutting parameters for obtaining higher cutting efficiency or accuracy in WEDM is still not fully solved, even with the most up-to-date CNC WEDM machine. This is mainly due to the nature of the complicated stochastic process mechanisms in wire EDM. As a result, the relationships between the cutting parameters and the process performance are hard to model accurately. Literature lacks much to say about the use of wire EDM for machining cylindrical forms (CWEDT) of a AISI D3 tool steel material, so the need has been felt towards the highlighting of this process with the goal of achieving mathematical models to enhance the process performance. The present work highlights the development of mathematical models for correlating the inter-relationships of various CWEDT machining parameters of AISI D3 material, such as power, pulse off-time, voltage, and spindle rotational speed on the surface roughness and roundness. This work has been established based on the response surface methodology (RSM) approach. Mathematical models fitted to the experimental data will contribute towards the selection of the optimum process conditions. Also, this study investigates the surface roughness and roundness of turning parts via the CWEDT process and explores possible ways to adjust its parameters to achieve better surface roughness and roundness by statistical methods. There are many ways to design a test, but the most frequently used approach is a full factorial experiment. However, for full factorial experiments, there are 3^f possible combinations that must be tested (f = the number of factors each at three levels). Therefore, it is very time consuming when there are many factors [18]. In order to minimize the number of tests required, fractional factorial experiments (FFEs) were developed. FFEs use only a portion of the total possible combinations to estimate the effects of main factors and the effects of some of the interactions. Taguchi developed a family of FFE matrices which could be utilized in various situations. These matrices reduce the experimental number but still obtain reasonably rich information. The conclusions can also be associated with statistical level of confidence. In Taguchi's methodology, all factors affecting the process quality can be divided into two types: control factors and noise factors [18]. Control factors are those set by the manufacturer and are easily adjustable. These factors are most important in determining the quality of

Table 2 Factor and factor levels of non-variable parameters in this experimentation

Factors	Factor levels		
	1	2	3
Power (level of current, A)	10	11	–
Pulse off-time (μs)	6	8	10
Voltage (V)	100	110	120
Spindle rotational speed (rpm)	16	45	–

Table 3 Non-variable parameters used in this experimentation

Factors	Factor levels
Max feed rate (mm/min)	1
Servo (V)	50
Wire tension (kg)	16
Wire speed (mm/s)	8
Dielectric	31
Inverse, finish	Off

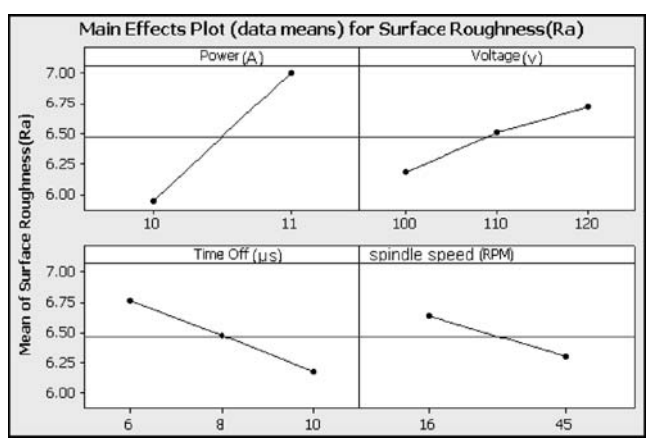

Fig. 4 Effects of factors on surface roughness (R_a values are in micrometer)

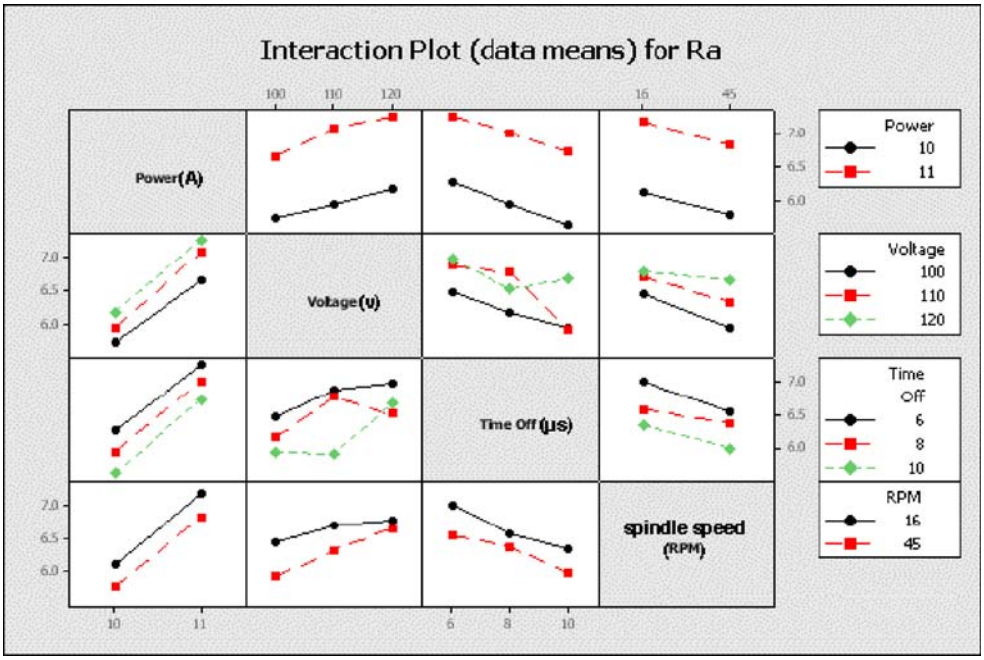

Fig. 5 Interaction effects on surface roughness (R_a values are in micrometer)

product characteristics. Parametric optimization in CWEDT is to find out the main control factors and select their appropriate levels. The important strength of factorial design of experiments (DOE) is the potential to build models and to gradually increase the complexity of the models if this is needed. In addition, a good combination between factorial DOE and the Taguchi method is the use of factorial design but with an emphasis on robustness, performing repetitions and various levels of noise factors as proposed by Taguchi. In order to determine prediction model, one can first use Taguchi methods to determine a working space with high robustness, and then use factorial designs to generate a model of high stability [19]. Full factorial technique is used widely in DOE lately and is employed here to perform the experimental design [20]. Three different analyses are performed on the data obtained from experiments where the interpretation of their results is of great importance in any experimental

Table 4 Analysis of variance for surface roughness (R_a)

Source	DF	Seq SS	Adj SS	Adj MS	*F*	*P*
Power	1	20.2621	20.2621	20.2621	120	0
Voltage	2	3.463	3.463	1.7315	10.25	0
Pulse off-time	2	4.3096	4.3096	2.1548	12.76	0
Spindle rotational speed	1	2.1151	2.1151	2.1151	12.53	0.001
Power × voltage	2	0.1399	0.1399	0.07	0.41	0.664
Power × pulse off-time	2	0.0372	0.0372	0.0186	0.11	0.896
Power × spindle rotational speed	1	0.0081	0.0081	0.0081	0.05	0.828
Voltage × pulse off-time	4	2.2543	2.2543	0.5636	3.34	0.02
Voltage × spindle rotational speed	2	0.4636	0.4636	0.2318	1.37	0.266
Pulse off-time × spindle rotational speed	2	0.2174	0.2174	0.1087	0.64	0.531
Power × voltage × pulse off-time	4	1.1097	1.1097	0.2774	1.64	0.185
Power × voltage × spindle rotational speed	2	0.6475	0.6475	0.3237	1.92	0.162
Power × pulse off-time × spindle rotational speed	2	0.3073	0.3073	0.1537	0.91	0.412
Voltage × pulse off-time × spindle rotational speed	4	0.3923	0.3923	0.0981	0.58	0.678
Power × voltage × time-off × spindle rotational speed	4	0.63	0.63	0.1575	0.93	0.456
Error	36	6.0789	6.0789	0.1689		
Total	71	42.436				

Table 5 Table of R^2 and R_{adj}^2 test for regression model for R_a

Degree	R-Sq (%)	R-Sq(adj) (%)
Linear	70.9	69.2
Linear + squares	71	68.4
Linear + interaction	72.6	68.1
Full quadratic	72.2	67.2

work. Firstly, analysis of variance (ANOVA) is run which helps one to determine significant factors and factors interactions. Secondly, regression analysis establishes a relationship between factors and responses. Finally, analysis of variance for regression is used to determine the accuracy of the regression model [19]. Scanning electron microscopy (SEM) has been a common tool to examine EDM surfaces. The EDM surface consists of small craters, sub-surface recast layer, and HAZ created by electrical sparks. To improve the EDM surface integrity, the size of craters needs to be small [3]. In this research, SEM and microhardness tests are used to examine and investigate the sub-surface recast layers and HAZ of machined parts under specific process parameters.

2 Experimental setup

The equipment used in order to carry out the EDM process was a wire EDM machine of type ONA R250 CNC. The wire EDM machine was equipped with a rotary axis in order to produce cylindrical forms (Fig. 2). The experiments are aimed at considering the effects of several controllable factors on surface roughness and roundness. The surface finish was measured using a mobile roughness measurement (Mahr Perthometer M2) with a 0.8-mm cut off length (according to DIN EN ISO274:1998), and the roundness of machined parts was measured using a coordinate measuring machine (ZEISS Prismo 5 CMM). The microhardness of machined parts was measured using Leitz Wetzlar Germany instrument. The straight turning configuration is used during this study. The specimens chosen in this case were AISI D3 tool steel punches due to their growing range of applications in the field of manufacturing dies and molds (Fig. 3). Hardness of work pieces (with 10 mm diameter) was 62±2 HRC. Depth and length of cut in all experiments were 2 and 10 mm, respectively. The chemical composition of workpieces is shown in Table 1. In this research, the AISI D3 tool steel cylindrical parts were machined using 0.25 mm diameter brase wire (63%Cu–37%Zn). The wire–workpiece gap usually ranges from 0.025 to 0.075 mm and is constantly maintained by a computer-controlled positioning system.

Table 6 Table of regression model for R_a

Term	Coefficient	SE coefficient	T	P
Constant	−6.04139	1.29149	−4.678	0
Power	1.06098	0.10116	10.488	0
Voltage	0.02664	0.00619	4.301	0
Pulse off-time	−0.14981	0.03097	−4.837	0
Spindle rotational speed	−0.01182	0.00349	−3.389	0.001
S=0.4292	R-Sq=70.9%		R-Sq(adj)=69.2%	

Table 7 ANOVA table for regression analysis for R_a

Source	DF	Seq SS	Adj SS	Adj MS	F	P
Regression	4	30.094	30.094	7.5235	40.84	0
Linear	4	30.094	30.094	7.5235	40.84	0
Residual error	67	12.342	12.342	0.1842		
Lack-of-fit	31	6.263	6.263	0.202	1.2	0.3
Pure error	36	6.079	6.079	0.1689		
Total	71	42.436				

3 Design of experiments

According to initial tests done by Mohammadi et al. [4, 12] using the Taguchi approach in DOE with the application of $L_{18}(2^1 \times 3^7)$ standard orthogonal array and primary tests accomplished on AISI D3 tool steel specimens by the authors using ONA Aricut R250 technology manual and user's guide, and $L_9(3^4)$ Taguchi standard orthogonal array, factors and factor levels were selected for determining optimal process setting conditions, significant factors, and their interactions (Table 2). Power, pulse off-time, voltage, and spindle rotational speed are adopted as factors (independent variables) which vary during the experiments. Also non-variable factors are presented in Table 3. These factors are set apart from the experiment, and they are neither presumed to have important effect on the process, nor can vary because of the equipment setup [4, 12]. One of the most used techniques for the design of experiments is the factorial design, which consists of experimenting with all the possible combinations of variables and levels. If the number of the design factors' level is different, a kind of full factorial design, mixed level design, is used. These mixed level factorial designs are among the most widely used types of designs for process design and process improvement. In this research, a mixed level design of $2^2 \times 3^2$ was designed for experimentation. Thus, 36 experiments were conducted with parameter levels shown in Table 2. Each run is replicated two times so that the total

Table 8 Results of confirmation tests for R_a

Run	Power	Voltage	Pulse off-time	Spindle rotational speed	Results of model (R_a)	Results of experiments (R_a)	Regression error (%)
1	11	120	6	16	7.74	7.48	3.4
2	10	100	10	45	5.2	5.2	0
3	11	110	8	45	6.83	6.872	−0.6
4	12	105	12	90	6.63	6.78	−2.2

number of runs was 72. The resolution of this factorial design allows us to estimate all the main effects and factor interactions in this study. Note that the experiments were run in random order using randomization table, even the repetition of each run was not done, respectively.

4 Data analysis

4.1 Analysis of surface roughness

Figures 4 and 5 depict the plots of factor effects and interaction effects on surface roughness, respectively. Note that data mean value is used to determine each factor's effect. Figure 4 serves the purpose of graphical assessment. Figure 4 shows that power, voltage, pulse off-time, and spindle rotational speed have the most significant effect on R_a. In addition, power has direct proportion to the surface roughness; that is, by increasing power, surface roughness increases significantly. Also, it is indicated from Fig. 4 that voltage has a significant effect on surface roughness because in the lower voltage, by increasing in voltage value, R_a increases strongly but in higher values of voltage, R_a increases slowly. As indicated in Fig. 4, pulse off-time and spindle rotational speed have reverse effects on surface roughness. ANOVA is numerously employed by experimenters since it covers the shortcomings of graphical assessment. Two of these shortcomings are inaccuracy in the inferences made and that the inferences are only comparatively valid. In Table 4, the ANOVA table for surface roughness is presented. Power, voltage, pulse off-time, spindle rotational speed, and the interaction between the voltage and pulse off-time are the factors which present a P value lower than α level of confidence [18]. So, it is inferred that only the abovementioned factors and interaction effects have a significant impact on surface roughness among all others.

Equation 1 presents the linear relationship between factors, factor effects, and surface roughness (response) which is the result of response surface regression analysis.

$$R_a\ (\mu\text{m}) = -6.04139 + 1.06098 \times \text{Power} + 0.02664 \times \text{Voltage} - 0.14981 \times \text{Pulse off time} - 0.01182 \times \text{Spindle rotational speed} \quad (1)$$

Table 5 indicates that the regression model is the best one in comparison with the others that can be used with these factors and factor levels by R_{adj}^2 test (The R-Sq (R^2) value indicates that the predictors explain 70.9% of the variance in R_a). The R-Sq (adj) (R_{adj}^2) is 69.2%, which accounts for the number of predictors in the model. Both values indicate that the model fits the data well. Table 6 shows the coefficients of factors and factor effects in the regression model. Table 7 shows the ANOVA table for

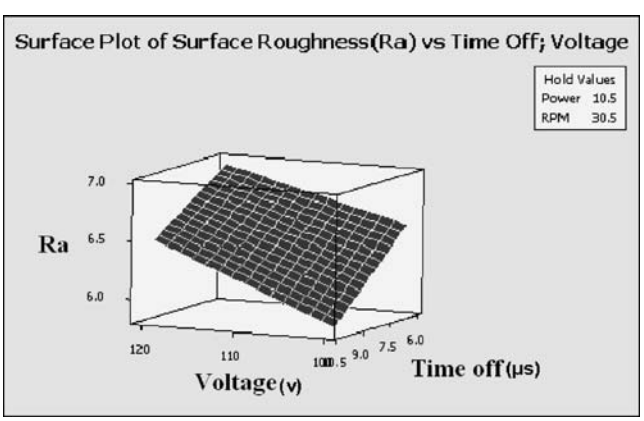

Fig. 6 Estimated response surface of R_a vs. voltage and pulse off-time (R_a values are in micrometer)

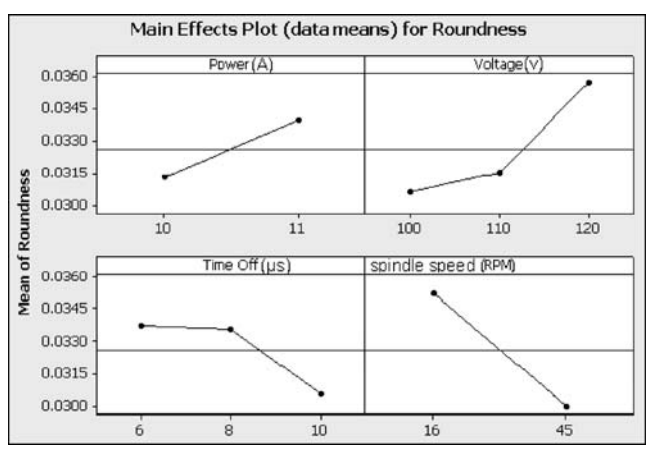

Fig. 7 Effects of factors on roundness (roundness values are in micrometer)

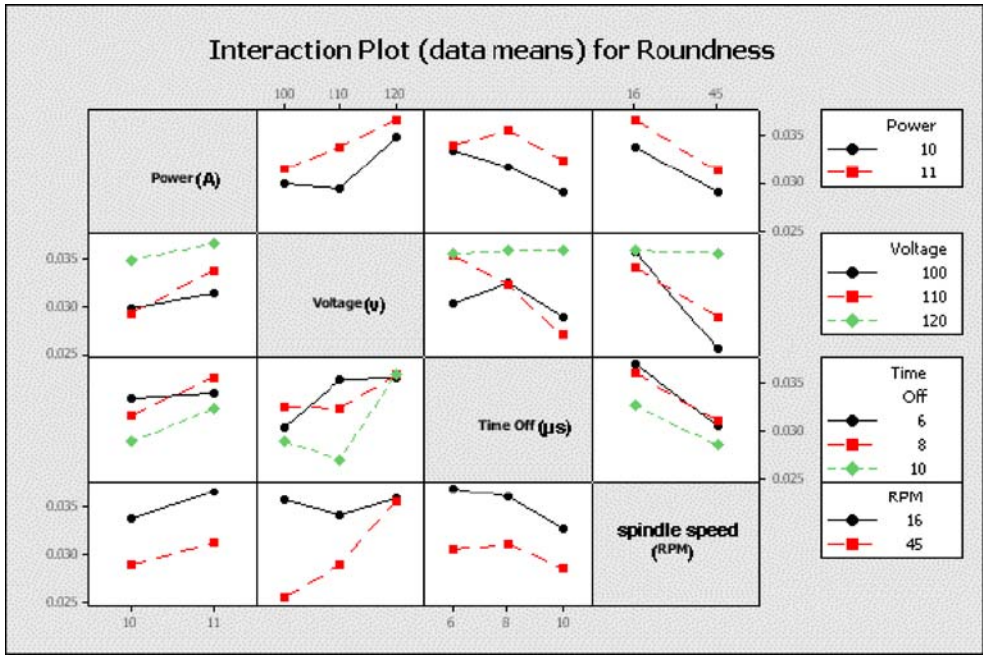

Fig. 8 Interactions of factors on roundness (roundness values are in micrometer)

regression analysis. This table indicates that the model estimated by the regression procedure is significant at an α level of 0.05. Table 8 shows verification of the test results. The predicted machining parameter performance was compared with the actual machining performance, and a good agreement was obtained between these performances. The above regression equation for surface roughness of CWEDT is of great importance to the proper selection of machining parameters during the machining of the cylindrical parts.

Figure 6 presents response surface of R_a vs. voltage and pulse off-time, whereas the other factors are held constant at their central values. It is indicated that by increasing the pulse off-time values and decreasing the voltage values, the amount of surface roughness is minimized, while in the higher values of voltage by increasing the pulse off-time values, surface roughness decreases. Also, in the lower values of pulse off-time by decreasing the voltage values, surface roughness decreases.

Table 9 Table of ANOVA for roundness

Source	DF	Seq SS	Adj SS	Adj MS	*F*	*P*
Power	1	0.000125	0.000125	0.000125	4.47	0.042
Voltage	2	0.000361	0.000361	0.00018	6.46	0.004
Pulse off-time	2	0.000152	0.000152	7.59E−05	2.72	0.079
Spindle rotational speed	1	0.000495	0.000495	0.000495	17.74	0
Power × voltage	2	2.76E−05	2.76E−05	1.38E−05	0.49	0.614
Power × pulse off-time	2	3.99E−05	3.99E−05	0.00002	0.72	0.496
Power × spindle rotational speed	1	1.5E−06	1.5E−06	1.5E−06	0.05	0.817
Voltage × pulse off-time	4	0.000186	0.000186	4.66E−05	1.67	0.178
Voltage × spindle rotational speed	2	0.000299	0.000299	0.00015	5.37	0.009
Pulse off-time × spindle rotational speed	2	1.72E−05	1.72E−05	8.6E−06	0.31	0.737
Power × voltage × pulse off-time	4	5.64E−05	5.64E−05	1.41E−05	0.51	0.732
Power × voltage × spindle rotational speed	2	2.14E−05	2.14E−05	1.07E−05	0.38	0.685
Power × pulse off-time × spindle rotational speed	2	5.31E−05	5.31E−05	2.66E−05	0.95	0.395
Voltage × pulse off-time × spindle rotational speed	4	0.000114	0.000114	2.85E−05	1.02	0.409
Power × voltage × pulse off-time × spindle rotational speed	4	7.31E−05	7.31E−05	1.83E−05	0.65	0.627
Error	36	0.001004	0.001004	2.79E−05		
Total	71	0.003026				

Table 10 Table of regression model for roundness

Term	Coefficient	SE Coefficient	*T*	*P*
Constant	0.046354	0.022612	2.05	0.044
Power	0.002631	0.001186	2.219	0.03
Voltage	−0.00027	0.000169	−1.587	0.117
Pulse off-time	−0.00079	0.000363	−2.18	0.033
Spindle rotational speed	−0.00208	0.000552	−3.757	0
Voltage × spindle rotational speed	0.000017	0.000005	3.439	0.001
S=0.005030	R-Sq=44.8%		R-Sq(adj)=40.6%	

4.2 Analysis of roundness

Figures 7 and 8 depict the plots of factor effects and interaction effects on roundness, respectively. Note that data mean is used to determine each factor's effect. Figure 7 serves the purpose of graphical assessment. Figure 7 shows that the most influential factor over roundness is spindle rotational speed, in such a way that the value of the roundness decreases greatly when spindle rotational speed is increased. With regard to the power and voltage factors, as it is shown in Fig. 7, the value of roundness tends to increase when these factors are increased, but the effect of voltage on the roundness is much higher. The effect of pulse off-time on roundness is lower than others. Figure 7 shows that with the increase in pulse off-time value, roundness decreases, especially in the higher values of pulse off-time.

In Table 9, the ANOVA table for roundness is presented. Spindle rotational speed, voltage, and power are the factors which present a *P* value lower than α level of confidence. Also, it is inferred that only the interaction effect between voltage and spindle rotational speed has a significant impact on roundness among all other interaction effects.

Equation 2 presents the relationship between factors and roundness (response) which is the result of response surface full quadratic regression analysis.

Table 11 ANOVA table for regression analysis for roundness

Source	DF	Seq SS	Adj SS	Adj MS	*F*	*P*
Regression	5	0.001356	0.001356	0.000271	10.72	0
Linear	4	0.001056	0.001035	0.000259	10.22	0
Interaction	1	0.000299	0.000299	0.000299	11.83	0.001
Residual error	66	0.00167	0.00167	0.000025		
Lack-of-fit	30	0.000666	0.000666	0.000022	0.8	0.737
Pure error	36	0.001004	0.001004	0.000028		
Total	71	0.003026				

Table 12 Results of confirmation tests for roundness

Run	Power	Voltage	Pulse off-time	Spindle rotational speed	Results of model	Results of experiments	Regression error (%)
1	11	120	6	16	0.0375	0.035	7.19
2	10	100	10	45	0.0207	0.022	−5.43
3	11	110	8	45	0.0298	0.031	−2.26

$$\begin{aligned}\text{Roundness } (\mu\text{m}) = {} & 0.046354 + 0.002631 \times \text{Power} \\ & - 0.00027 \times \text{Voltage} - 0.00079 \\ & \times \text{Pulse off time} - 0.00208 \\ & \times \text{Spindle rotational speed} \\ & + 0.000017 \times \text{Voltage} \\ & \times \text{Spindle rotational speed} \end{aligned} \quad (2)$$

Table 10 indicates that the regression model is the best one in comparison with the others that can be used with these factors and factor levels by R_{adj}^2 test. The R-Sq (R^2) value indicates that the predictors explain 44.8% of the variance in material removal rate. The R_{adj}^2 value is 40.6%, which accounts for the number of predictors in the model. Both values indicate that the model fits the data well. Also this table shows the coefficient of factors and factor effects in the regression model. Table 11 shows the ANOVA table for regression analysis. This table indicates that all terms of the model estimated by the regression procedure are significant at an α level of 0.05. Table 12 shows verification of the test results. The predicted machining parameter performance was compared with the actual machining performance, and a good agreement was obtained between these performances.

Figure 9 shows the estimated response surface of roundness as a function of the factors of voltage and spindle rotational speed, while the pulse off-time and power remain constant in their central values. This figure shows that by increasing the spindle rotational speed and decreasing the voltage values, the roundness values are minimized. It is clearly seen that in the higher values of voltage, the influence of spindle rotational speed is limited, but in the lower values of voltage, by increasing in the spindle rotational speed values, the roundness values decrease strongly. As can be clearly seen in this figure, in the higher values of spindle rotational speed, by increasing the voltage values, the roundness values increases.

Figure 10 shows the estimated response of roundness, varying the factors of voltage and pulse off-time. As can

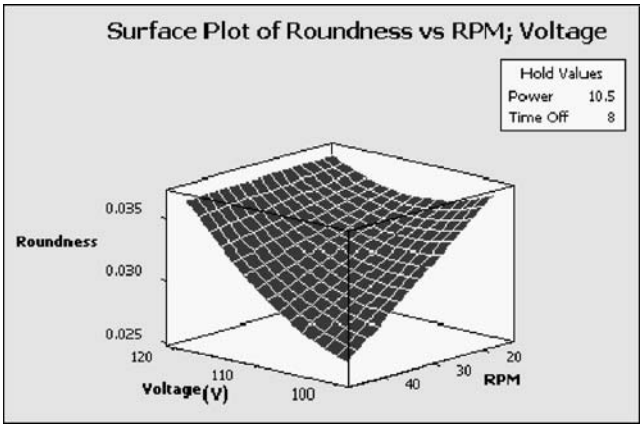

Fig. 9 Estimated response surface of roundness vs. voltage and spindle rotational speed (roundness is in micrometer)

be clearly seen in this figure, by increasing the voltage and decreasing the pulse off-time values, the roundness maximizes. The higher values of pulse off-time and lower values of voltage redound the lowest values of roundness. Furthermore, in the lower values of pulse off-time, by decreasing the voltage values, the roundness decreases. Also, in the higher values of voltage, by increasing the pulse off-time values, the roundness decreases.

Figure 11 shows the estimated response surface of roundness as a function of the factors of voltage and power, while the pulse off-time and spindle rotational speed remain constant in their central values. This figure shows that by decreasing the power and voltage values, the roundness value minimizes. It indicates that in the higher values of voltage, by increasing the power value, the roundness decreases. Also, in the higher values of power, by decreasing the voltage value, roundness decreases.

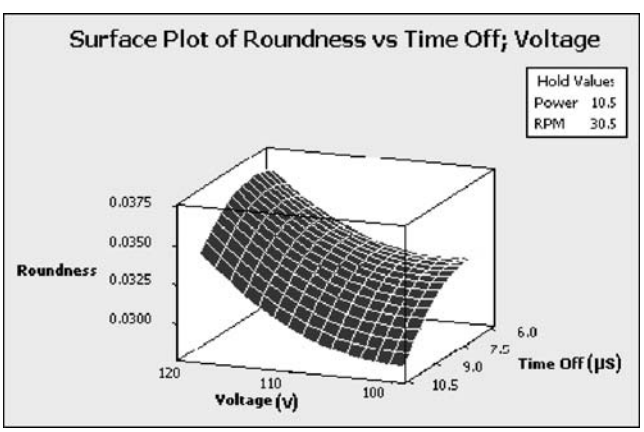

Fig. 10 Estimated response surface of roundness vs. voltage and pulse off-time (roundness is in micrometer)

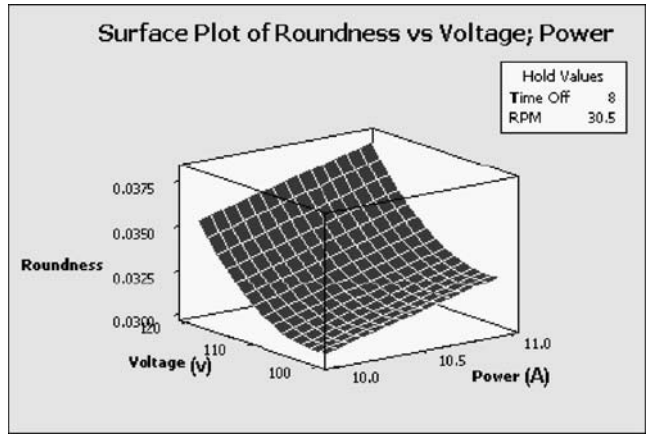

Fig. 11 Estimated response surface of roundness vs. voltage and power (roundness is in micrometer)

5 Discussion

In this present work, modeling procedures of two of the most important parameters within the process of CWEDT were carried out. The material chosen in this study was a AISI D3 tool steel due to its growing range of applications in the field of tools, dies, and molds as a punch, deep drawing, tapping, reaming, and so on in cylindrical forms. With this work, it has been confirmed that the technique of design of factorial experiments, combined with the techniques of RSM, can be successfully applied to modeling the functions which depend on various variables. In order to carry out this study, two technological variables, such as surface roughness (evaluated by means of the R_a parameter) and roundness, were selected. These technological variables were studied in relation to design factors such as the level of power supplied by the WEDM machine generator (level

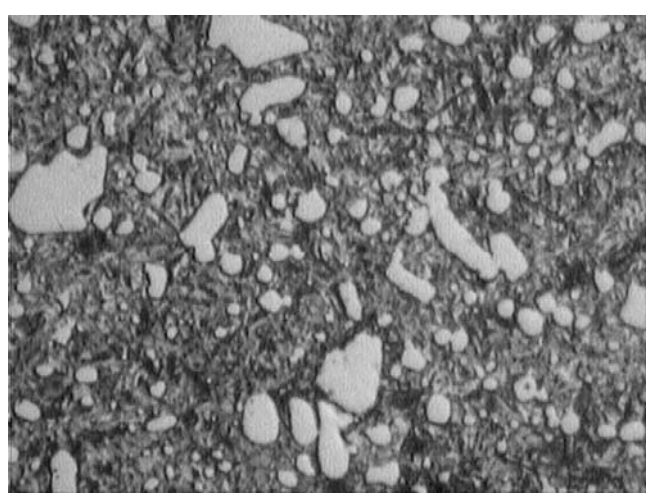

Fig. 12 Metallographic graph of the microstructure of AISI D3 tool steel (magnification=500×)

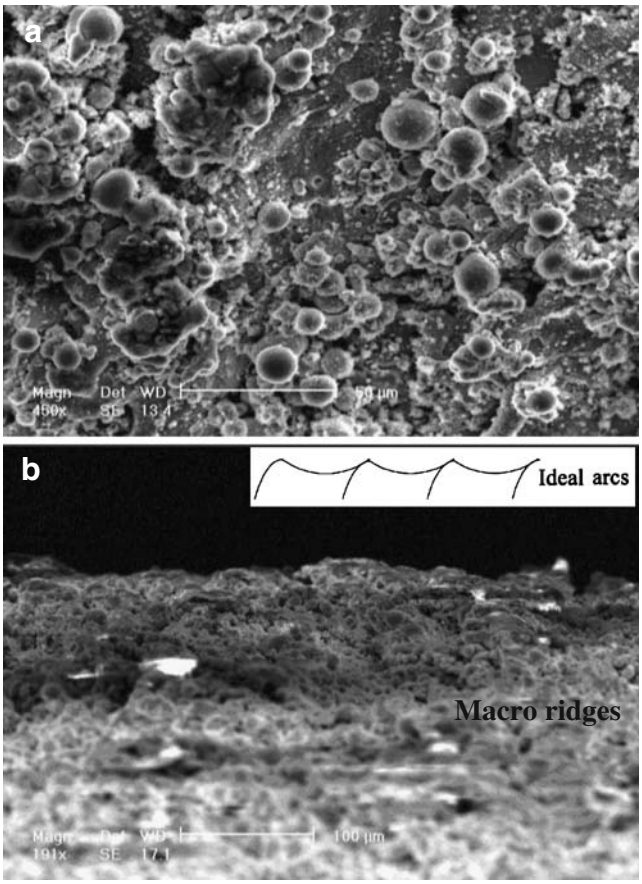

Fig. 13 **a** SEM micrographs of EDMed surface. **b** SEM micrographs of macro-ridges and ideal arcs on machined surface (under high MRR=14.916 and R_a=7.48: power=11 A, voltage=120 V, pulse off-time=6 μs, spindle rotational speed=16 rpm, magnification =450× and 191×)

of current), voltage, pulse off-time, and spindle rotational speed. In all the response variables used in this work, the mathematical model was derived. In the case of the surface roughness performance, the most influential factors were power, voltage, pulse off-time, and spindle rotational speed followed by the interaction effects between voltage and spindle rotational speed. When either power or voltage was increased, the roughness value also increased. Therefore, in order to obtain a good surface finish in the case of CWEDT, low values should be used for both power and voltage. Another way of obtaining low roughness values, although higher in previous cases, is to combine the use of high values of voltage and high values of pulse off-time, within the considered work interval. In the case of roundness, it was also seen that the spindle rotational speed was the most influential, followed by the interaction effect of voltage and spindle rotational speed. In order to be able to obtain low values of roundness, values of the voltage factor close to its central value or slightly higher should be used along with high values for spindle rotational speed, within the considered work interval. SEM is used to examine the surface integrity and sub-surface of CWEDT AISI D3 tool steel. The cylindrical samples were sliced in the radial direction. The surfaces of sliced cross sections were polished and etched to observe the sub-surface damage. Although regular EDMed surfaces are isotropic and have no specific texture or pattern, CWEDT surfaces may have macro-ridges, or circular arcs, in the cross section [3]. Figure 12 shows the metallurgical graph of the microstructure of AISI D3 tool steel specimens. It can be seen that there are a lot of coarse chromium carbides in the field of microstructure. Figures 13, 14, and 15 show the surfaces of three CWEDT parts.

As it is indicated in Figure 13, in high material removal rate conditions, discharge energy is released by increasing the power and voltage values and lowering pulse off-time. Therefore, the molten material of the workpiece surface has high fluency. In this case, because of high cooling rate, the big spherical grains can grow in order to subtract the surface energy. In this case, the surface roughness is high basically. Figure 14 shows that in low voltage and power values and higher pulse off-time, the feasibility of big

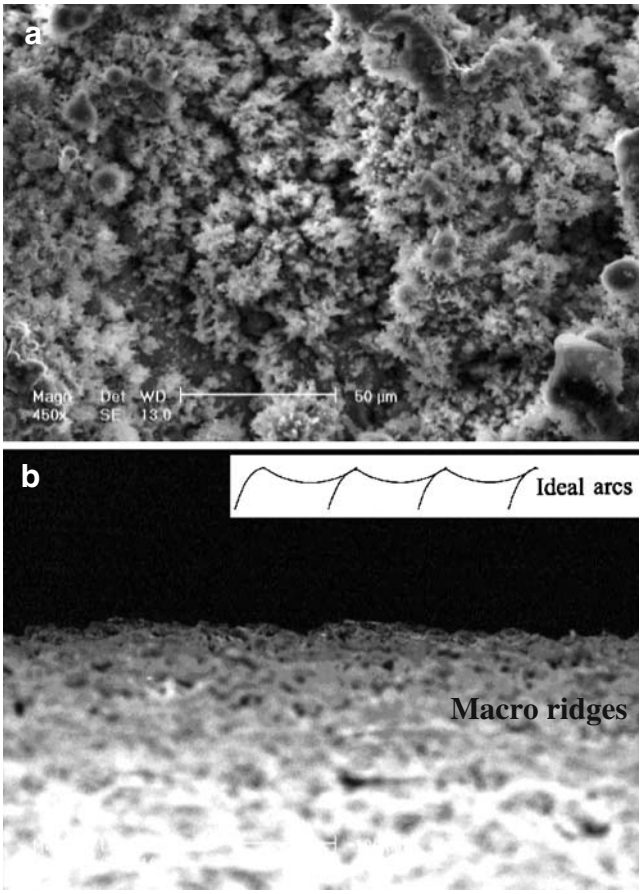

Fig. 14 **a** SEM micrographs of EDMed surface. **b** SEM micrographs of macro-ridges and ideal arcs on machined surface (under low MRR=10.453 and R_a=5.2: power=10 A, voltage=100 V, pulse off-time=10 μs, spindle rotational speed=45 rpm, magnification =450× and 191×)

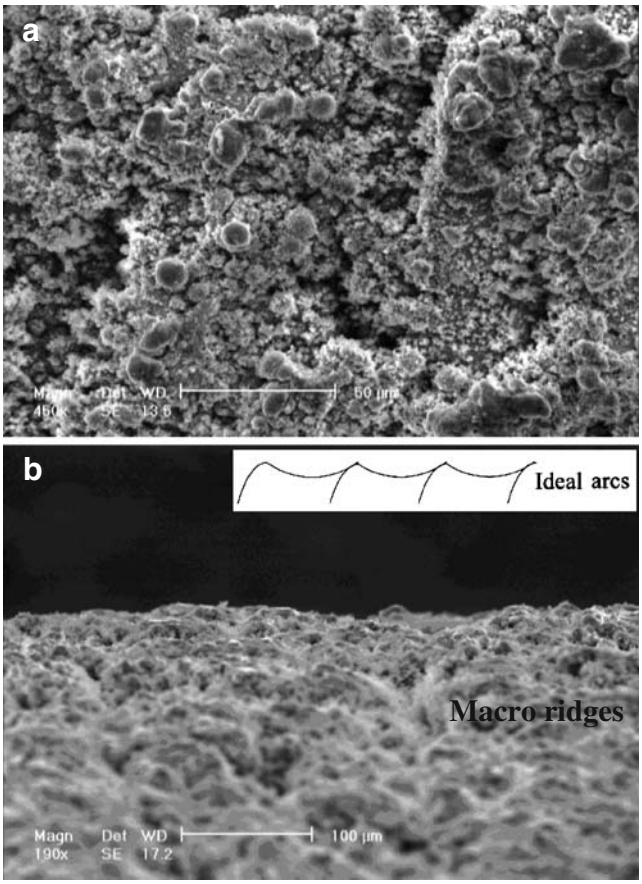

Fig. 15 **a** SEM micrographs of EDMed surface. **b** SEM micrographs of macro-ridges and ideal arcs on machined surface (under medium discharge energy: power=11 A, voltage=110 V, pulse off-time=8 μs, spindle rotational speed=45 rpm, magnification =450× and 191×)

spherical grains does not exist. This causes the smaller roughness and higher adherence in the surface. Figure 15 proves the above pretension, which indicates the EDM surface in medium discharge energy. The recast layer is defined as the material melted by electrical sparks and resolidified on the surface without being ejected nor removed by flushing. Below the recast layer is the HAZ. For the tool steel material, the chromium carbide melts and resolidifies in the HAZ. The molten chromium carbide dissolved in the martensite base because of lower cooling rate; therefore, the chromium carbide grains have no time to grow and then this phase will be small. This is observed in the SEM micrograph cross section and is used to identify the depth of HAZ. In the recast layer, the solution of chromium carbide is complete and the final phase is martensite because of higher cooling rate of this area. Although regular EDM surfaces are isotropic and have no specific texture or pattern [3, 13], CWEDT surfaces may have macro-ridges, or circular arcs, in the cross section. Figures 13, 14, and 15 show the surfaces of three cylindrical wire EDM AISI D3 parts. These figures also show the ideal surfaces that consist of circular arcs with the same pitch and radius of the circular arc in the ideal surface that is equal to the radius of the wire plus the gap between wire and workpiece [3]. These SEM micrographs also verify the surface finish model described in [3].

SEM micrographs of the cross section of the tool steel parts machined under both high and low material removal rate experiments are shown in Figs. 16 and 17. The recast layer, craters in the recast layer, and HAZ of two tool steel samples are presented in Figs. 16 and 17. Under high material removal rate, the recast layer, about 40–50 μm thick is clearly observed on the surface. Thinner recast layers, less than 15–20 μm, exist on samples machined by

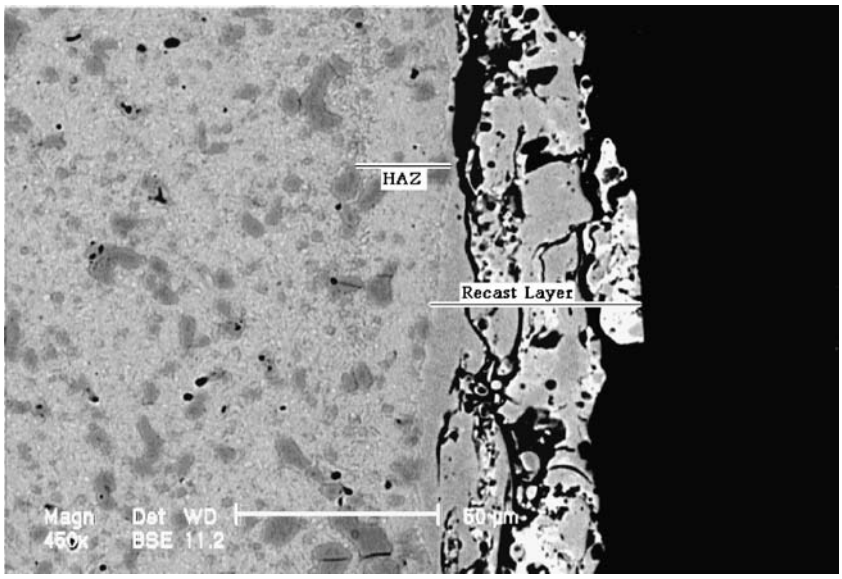

Fig. 16 SEM micrographs of surfaces and cross sections under high MRR=14.916 and R_a=7.48 (power=11 A, voltage=120 V, pulse off-time=6 μs, spindle rotational speed=16 rpm)

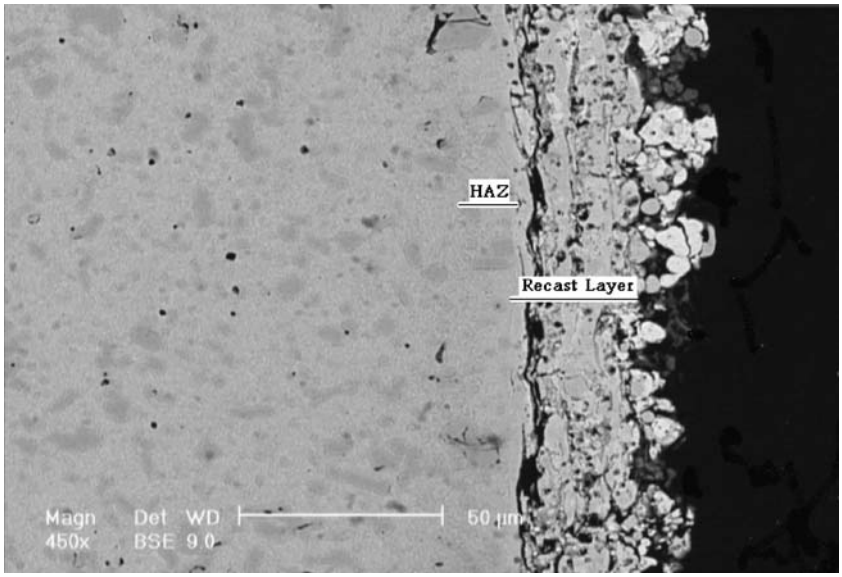

Fig. 17 SEM micrographs of surfaces and cross sections under low MRR=10.453 and R_a=5.2 (power=10 A, voltage=100 V, pulse off-time=10 µs, spindle rotational speed=45 rpm)

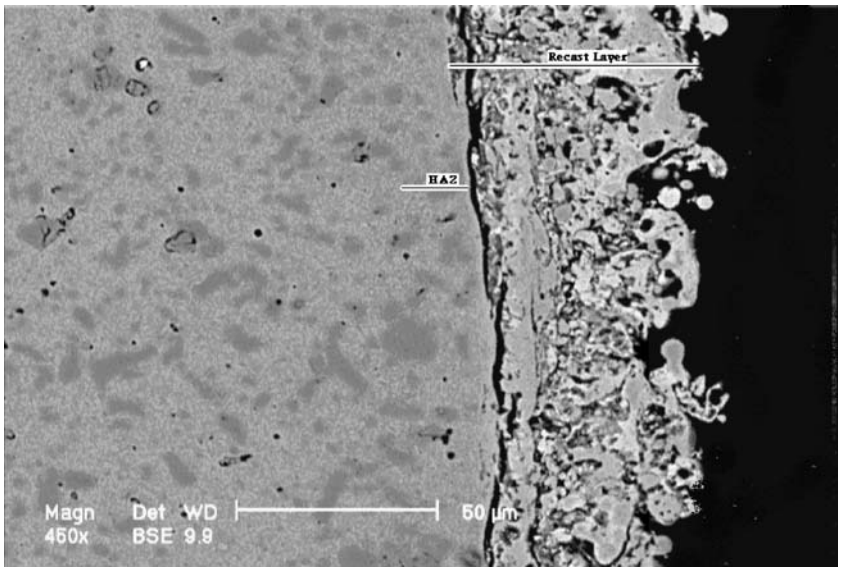

Fig. 18 SEM micrographs of surfaces and cross sections under medium discharge energy (power=11 A, voltage=110 V, pulse off-time=8 µs, spindle rotational speed=45 rpm)

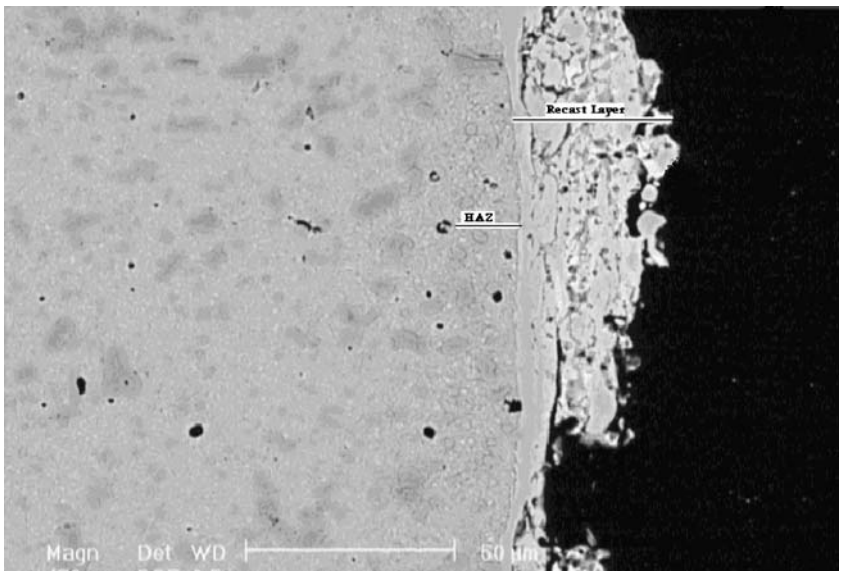

Fig. 19 SEM micrographs of surfaces and cross sections (power=12 A, voltage=105 V, pulse off-time=12 µs, spindle rotational speed=90 rpm)

Table 13 Results of microhardness measurement

Factors					Results of experiments		Microhardness results (HV)	
Run	Power	Voltage	Pulse off-time	Spindle rotational speed	MRR	R_a	HAZ	Bulk material
1	11	120	6	16	14.92	7.48	696.66	946
2	10	100	10	45	9.475	5.2	818.75	946
3	11	110	8	45	11.95	6.87	661.33	946
4	12	105	12	90	10.45	6.78	716.5	946

lower material removal rate conditions. As shown in Figs. 16 and 17, the depth of the heat-affected zone is estimated to be about 20–25 and 8–13 μm on the two samples with high and low material removal rate, respectively. Also, Figs. 18 and 19 show the cross section of EDM surfaces under medium discharge energy. It can be seen from Fig. 19 that the discharge energy is lower than the experiment shown in Fig. 18. The microhardness of sample 1 with the highest material removal rate and sample 2 with the best surface roughness were measured by an optical microscope. The hardness of HAZ and the bulk material was measured. The load during measuring the microhardness was 981 mN. Table 13 shows the results of the microhardness measurement. It can be seen that the hardness values have decreased in the HAZ. In the HAZ, the carbide grains melt and resolidify by high cooling rate. In this case, the carbide grains have no time to grow and sediment in the martensite basis, with small grains. It can be seen from Table 13 that by increasing the discharge energy the grains grow slowly, and therefore, the hardness of the HAZ decreases. Discharge energy is an important EDM process parameter that affects the thickness of the recast layer and HAZ. Higher power and voltage with lower pulse off-time generate higher discharge energy. The material removal rate is, in general, higher for the higher discharge energy.

EDAX SEM was used to identify the elements in three regions: bulk material, heat-affected zone, and recast layer. The bulk material and heat-affected zone had similar EDAX SEM analysis results, as shown in Fig. 20a, where Fe, Cr, and C were present in the two regions. Figure 20b shows that two additional elements, Cu and Zn, were detected in the recast layer. This can be explained by the melting and resolidification of the brass wire electrode during EDM spark erosion. In this study, the AISI D3 tool steel cylindrical part was machined using 0.25 mm diameter brass wire (63%Cu–37%Zn). As it is indicated in Fig. 20b, the amount of Cu element in the recast layer is higher than Zn because in the discharge temperature it evaporates.

6 Conclusions

The effects of machining parameters on the surface roughness and roundness values of machined components by CWEDT have been investigated experimentally. The

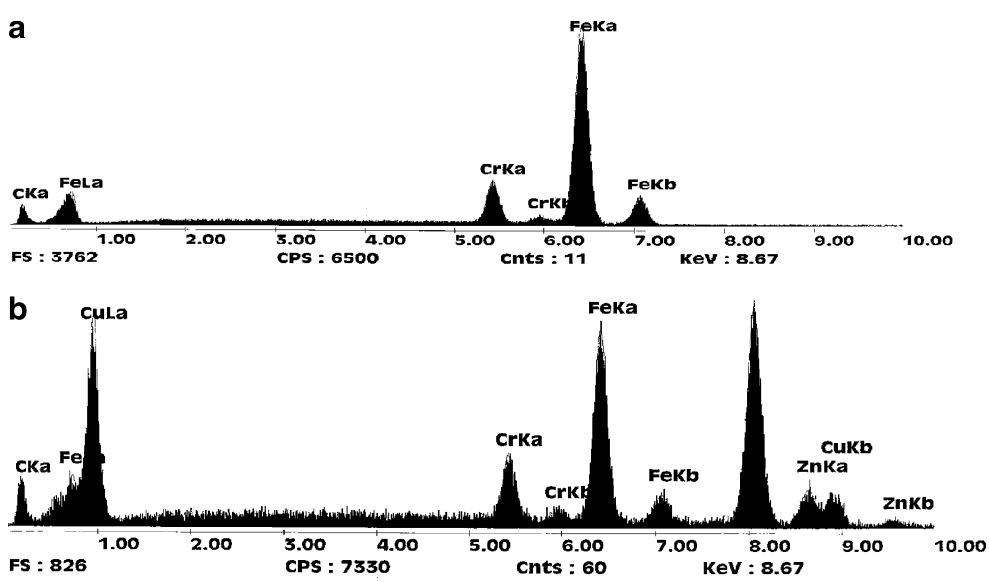

Fig. 20 EDAX SEM analysis. **a** Bulk material and heat-affected zone. **b** Recast layer

surface roughness is apparent to have an increasing trend with increase in the voltage and power and decrease in the pulse off-time and spindle rotational speed. This is mainly due to more discharge energy released during this time and expanding discharge channel. It is known that the diameter of the discharge channel is directly proportional to the pulse time off. Hence, craters with larger diameter are produced with shorter pulses time off, which in turn results in higher surface roughness values. A similar discussion may be applied for rougher surfaces with increasing discharge energy. Release of more energy during a fixed discharge duration results in the formation of craters with large diameter and higher depth. A response surface regression equation was found and presented as Eq. 1 for surface roughness.

Also, the level of importance of the machining parameters on the roundness is determined by using ANOVA. Based on the ANOVA method, the highly effective parameters on the roundness were found as spindle rotational speed, voltage, power, and interaction effects between voltage and spindle rotational speed, whereas pulse off-time was a less effective factor. The results showed that voltage and spindle rotational speed were more important than the power for controlling roundness. The regression model (relation) between the machining parameters and machining performance characteristic (roundness) is established as Eq. 2, and among the several functions tried, the linear and interaction model is found to be the best-fit model by using RSM.

The developed predictive models for the different machining performance characteristics of the CWEDT process are successfully proposed for proper selection of machining parameters for evaluation of surface roughness (R_a) and roundness under various machining combinations during the machining of the cylindrical parts by the CWEDT process. The ANOVA for regression analysis and confirmation tests indicates that the estimated models for surface roughness and roundness are significant. The macro-ridges, surface craters, recast layers, and heat-affected zones were observed, and their sizes were estimated using SEM.

References

1. Tosun N, Cogu C, Tosun G (2004) A study on kerf and material removal rate in wire electrical discharge machining based on Tagushi method. J Mater Process Technol 152:313–322
2. Qu J, Shih AJ, Scattergood RO (2002) Development of the cylindrical wire electrical discharge machining process, part 1: concept, design, and material removal rate. J Manuf Sci Eng 124 (3):702–707
3. Qu J, Shih AJ, Scattergood RO (2002) Development of the cylindrical wire electrical discharge machining process, part 2: surface integrity and roundness. J Manuf Sci Eng 124(3):708–714
4. A. Mohammadi, A. Fadaie Tehrani, E. Emanian, D. Karimi, H. Jafarpisheh, A new approach in turning by wire electrical discharge machining to evaluate the effects of machining parameters on MRR, in Tehran International Congress on Manuf. Eng, *Proc. TICME,* Tehran, Iran 12–15 Dec., 2005
5. Masuzawa T, Fujino M, Kobayashi K, Suzuki T (1985) Study on micro-hole drilling by EDM. Bull Jpn Soc Precis Eng 20(2):117–120
6. Masuzawa T, Kuo C-L, Fujino M (1994) A combined electrical machining process micronozzel fabrication. CIRP Ann 43:189–192
7. Masuzawa T, Tonshoff HK (1997) Three-dimensional micro-machining by machine tools. CIRP Ann 46:621–628
8. Rajurkar KP, Yu ZY (2000) 3D micro-EDM using CAD/CAM. CIRP Ann 49:127–130
9. Schoth A, Förster R, Menz W (2005) Micro wire EDM for high aspect ratio 3D microstructuring of ceramics and metals. Microsyst Technol 11:250–253
10. Rhoney BK, Shih AJ, Scattergood RO, Akemon JL, Grant DJ, Grant MB (2002) Wire electrical discharge machining of metal bond diamond wheels for ceramic grinding. Int J Mach Tools Manuf 42(12):1355–1362
11. Rhoney BK, Shih AJ, Scattergood RO, Ott R, McSpadden SB (2002) Wear mechanism of metal bond diamond wheels trued by wire electrical discharge machining. Wear 252(7–8):644–653
12. A. Mohammadi, A. Fadaie Tehrani, E. Emanian, D. Karimi, A new approach in surface roughness and roundness improvement in wire electrical discharge turning based on statistical analysis, in ASME International Conference on Manuf. Science & Eng., *Proc. ASME,* USA, Oct. 8–11, 2006
13. Rajurkar KP, Wang WM (1993) Thermal modelling and on-line monitoring of wire-EDM. J Mater Process Technol 38(1–2):417–430
14. Gokler MI, Ozanozgu AM (2000) Experimental investigation of effects of cutting parameters on surface roughness in the WEDM process. Int J Mach Tools Manuf 40(13):1831–1848
15. Tosun N, Cogun C, Inan A (2003) The effect of cutting parameters on workpiece surface roughness in wire EDM. Mach Sci Technol 7(2):209–219
16. Anand KN (1996) Development of process technology in wire-cut operation for improving machining quality. Total Qual Manag 7 (1):11–28
17. Spedding TA, Wang ZQ (1997) Parametric optimization and surface characterization of wire electrical discharge machining process. Precis Eng 20(1):5–15
18. Montgomery DC (2000) Design and analysis of experiments. Wiley, New York
19. M.J. Haddad, Statistical analysis of the results of the cylindrical wire electrical discharge turning process, M.Sc. dissertation, Mechanical Engineering Department, Isfahan University of Technology, Isfahan, Iran (2006) (in Persian)
20. Williams RE, Rajurkar KP (1991) Study of wire electrical discharge machined surface characteristics. J Mater Process Technol 28(1–2):127–138